

Journal of Biomedical Optics

SPIEDigitalLibrary.org/jbo

Porcine skin damage thresholds for 0.6 to 9.5 cm beam diameters from 1070-nm continuous-wave infrared laser radiation

Rebecca Vincelette
Gary D. Noojin
Corey A. Harbert
Kurt J. Schuster
Aurora D. Shingledecker
Dave Stolarski
Semih S. Kumru
Jeffrey W. Oliver

Porcine skin damage thresholds for 0.6 to 9.5 cm beam diameters from 1070-nm continuous-wave infrared laser radiation

Rebecca Vincelette,^{a,*} Gary D. Noojin,^a Corey A. Harbert,^a Kurt J. Schuster,^a Aurora D. Shingledecker,^a Dave Stolarski,^a Semih S. Kumru,^b and Jeffrey W. Oliver^b

^aTASC Inc., 4241 Woodcock Drive Suite B-100, San Antonio, Texas 78228

^b711th Human Performance Wing, Human Effectiveness Directorate, Bioeffects Division, Optical Radiation Bioeffects Branch, 4141 Petroleum Road, JBSA Fort Sam Houston, Texas 78234

Abstract. There is an increasing use of high-power fiber lasers in manufacturing and telecommunications industries operating in the infrared spectrum between 1000 and 2000 nm, which are advertised to provide as much as 10 kW continuous output power at 1070 nm. Safety standards have traditionally been based on experimental and modeling investigations with scant data available for these wavelengths. A series of studies using 1070-nm infrared lasers to determine the minimum visible lesion damage thresholds in skin using the Yucatan miniature pig (*Sus scrofa domestica*) for a range of beam diameters (0.6, 1.1, 1.9, 2.4, 4.7, and 9.5 cm) and a range of exposure durations (10 ms to 10 s) is presented. Experimental peak temperatures associated with each damage threshold were measured using thermal imaging. Peak temperatures at damage threshold for the 10-s exposures were $\sim 10^{\circ}\text{C}$ lower than those at shorter exposures. The lowest and highest experimental minimum visible lesion damage thresholds were found to have peak radiant exposures of 19 and 432 J/cm² for the beam diameter-exposure duration pairs of 2.4 cm, 25 ms and 0.6 cm, 10 s, respectively. Thresholds for beam diameters >2.5 cm had a weak to no effect on threshold radiant exposure levels for exposure times ≤ 0.25 s, but may have a larger effect on thresholds for exposures ≥ 10 s. © The Authors. Published by SPIE under a Creative Commons Attribution 3.0 Unported License. Distribution or reproduction of this work in whole or in part requires full attribution of the original publication, including its DOI. [DOI: 10.1117/1.JBO.19.3.035007]

Keywords: laser safety; damage threshold; infrared laser; minimum visible lesions; maximum permissible exposure; skin; Yucatan miniature pig; continuous wave laser; thermography; large beam diameter.

Paper 130805R received Nov. 8, 2013; revised manuscript received Feb. 18, 2014; accepted for publication Feb. 20, 2014; published online Mar. 21, 2014.

1 Introduction

The number of lasers in the operational range of 1000 to 2000 nm continues to increase in medical, industrial, communications, and military applications, while relatively few safety studies for skin damage from continuous-wave (CW) exposures at these wavelengths can be found in the literature. High-power fiber lasers utilize advanced technologies to combine active optical fibers with semiconductor diodes. These active fibers allow for an extremely high-intensity light out of a very small core, making it possible to produce multikilowatt lasers. For these lasers, powers >10 kW are routinely used in manufacturing processes and the telecommunications industry. CW outputs can be obtained with fiber lengths >100 m, with small beam divergence and high power conversion efficiencies. Experimental data used in setting the ANSI standards have not kept pace with the rapid advancement of these lasers. Furthermore, the maximum permissible exposure (MPE) recommended through the ANSI Z136.1-2007¹ is for a limiting, or measurement, aperture diameter of 0.35 cm in this wavelength region for exposures to skin with little empirical evidence that the standard recommendations are adequate for larger beam diameters, especially for highly penetrating wavelengths such as 1070 nm. Irradiances can easily exceed 10 kW/cm² and little or no minimum damage threshold data are available for these high levels.

Therefore, this study was initiated to answer critical questions regarding the appropriateness of the standards for MPE in terms of relative penetration depth (wavelength) and for CW lasers (10 ms to 10 s) with beam diameters greater than the ANSI limiting aperture of 0.35 cm in the near-infrared (IR) region at 1070 nm.

To determine if an MPE is sufficiently safe, a series of experiments are conducted to evaluate the damage threshold for a minimum visible lesion (MVL). An MVL is considered to be any subtle, slight, morphological, or coloration, change observed at the exposure site post laser radiation at various time points. The MPE is typically several times less than the MVL, to ensure that exposures at or below the MPE would have no damaging effects.

The Yucatan miniature pig has been established as a model for human skin damage studies due to the morphological and physiological similarities to human skin.² Skin threshold studies were conducted with Yucatan miniature pigs at wavelengths of 1070 and 1940 nm with varying spot sizes and exposure times. Results for the 1940-nm measurements have been reported³ while only portions of the 1070-nm data presented here have appeared previously.⁴ Also, MVL skin thresholds have been reported with these miniature pigs for various spot sizes and exposure times for wavelengths at 1318 and 1540 nm.⁵⁻⁷

A summary of threshold data obtained from the literature for skin exposure at 1060 nm are listed in Table 1. No published data were found for skin exposure at 1070 nm, which was used in this study, but optical properties of the skin are remarkably

*Rebecca Vincelette, E-mail: Rebecca.L.Vincelette.ctr@mail.mil

Table 1 Literature summary of skin damage threshold data at the 1060-nm laser wavelength.

Reference	Subject	Exposure time (s)	$1/e^2$ spot size (cm)	Damage threshold (J/cm^2)
10	White haired pig	1.0	0.5	59.4
10	Human—light complexion Chinese	1.0	0.5	65.5
10	Human—yellow complexion Chinese	1.0	0.5	61.0
10	Human—dark complexion Chinese	1.0	0.5	52.3
11	Human	1.0	0.5	71.4
12	Human	300×10^{-6}	0.5	20.3
13	Human	200×10^{-6}	0.5	9.9
14	Guinea pig—dark pigmented	10×10^{-9}	0.25	1.0
15	Human—Black	1	1.05	55°
15	Human—Caucasian	1	1.05	70°
15	Human—Black	75×10^{-9}	1.05	2.6°
15	Human—Caucasian	75×10^{-9}	1.05	7.5°

°Damage threshold calculated as the average for the radiant exposure of the lowest positive and highest negative responses 24 h post laser exposure.

similar between 1060 and 1070 nm, justifying direct comparison.^{8,9} The time of inspection used to assess damage endpoints is assumed to be 24 h post exposure; however, the exact time of evaluation for many of the studies was left ambiguous in the text and could range from immediate response to 48 h post exposure.

There are several chromophores in the skin related to the absorption, μ_a , of laser radiation at near-IR wavelengths. These chromophores include melanin, water, fat, hair, and blood. The values for μ_a have been reported by numerous sources and are summarized in Fig. 1.

The experiments reported in this study were designed to supplement and extend the body of knowledge summarized in Table 1 in the following ways: (1) To determine the MVL damage thresholds with beam spot size and exposure duration dependency, (2) to examine the thermal response on the surface of the skin over a variety of exposure conditions, and (3) to better understand the impact of the relative absorption coefficient (μ_a) of the skin on damage threshold for the deeply penetrating 1070-nm wavelength.

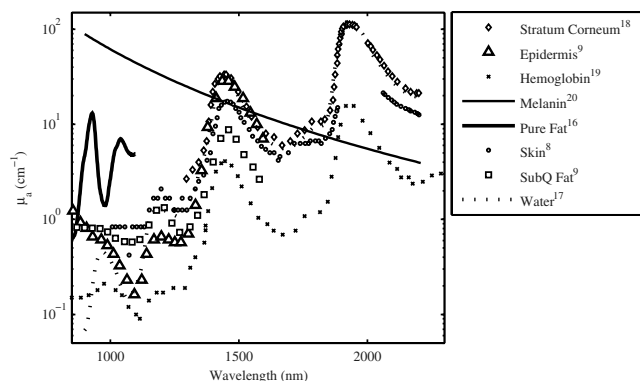


Fig. 1 Comparison of the absorption coefficient (μ_a) for various chromophores present in skin.^{8,9,16–20}

2 Methods

2.1 Animal Use

The animals involved in this study were procured, maintained, and used in accordance with the Federal Animal Welfare Act, “Guide for the Care and Use of Laboratory Animals,” prepared by the Institute of Laboratory Animal Resources National Research Council, and DoD Regulation 40-33 Secnavinst 3900.38C AFMAN 40-401(1) DARPAINST 18 USUHSINST 3203 “The Care and Use of Laboratory Animals in DOD Programs.” The Air Force Research Laboratory at Joint-Base Sam Houston, Texas, has been fully accredited by the Association for Assessment and Accreditation of Laboratory Animal Care, International since 1967.

A total of 22 female Yucatan miniature pigs were used for this study. Subjects had food withheld for 12 h prior to the procedure. Miniature pigs (30 to 50 kg) were sedated with an intramuscular (IM) injection of Tiletamine/Zolazepam (4 to 6 mg/kg) IM and Xylazine (2.2 mg/kg) IM. Subjects had an intravenous ear catheter (23 to 18 gauge) placed for the administration of lactated ringers. Animals were then orotracheally intubated and anesthesia was maintained with isoflurane (1 to 3%) throughout the procedure. Heart rate, oxygen saturation, core body temperature, and respiration were continuously monitored. After animals reached a surgical plane of anesthesia, electric clippers were used to remove hair from the flank. The flank was cleaned with soap and warm water, rinsed, and dried with a lint-free disposable cloth. The core body temperature of subjects was maintained using a T/Pump™ circulating water blanket (Gaymar Inc., Orchard Park, NY).

A grid pattern was drawn on the flank of the pigs using a black permanent marker with grid spacing of 1.5, 2, 3, 4, 8, or 12 cm for the nominal laser beam diameters of 0.6, 1, 2, 2.5, 5, and 10 cm, respectively. Skin biopsy punches (2 to 8 mm) were collected from select exposure sites at 1 and/or

24 h post exposure and stitched closed with nonabsorbable suture. Subjects were sedated again for 24 h post laser assessment and biopsies. Buprenorphine (0.05 to 0.1 mg/kg) was administered IM as a postprocedural analgesic.

For laser exposures, anesthetized pigs were placed in a customized pig sling (BH Inc., Wheatland, WY) or on a hydraulic table in ventral recumbence. In this manner, each area of the grid, which had been drawn on the flank of the pig, was sequentially addressed with a laser exposure, according to a predetermined randomized selection of energy levels distributed over a range encompassing the anticipated threshold. Energy readings for each laser exposure and any remarkable observations were recorded on data sheets following each exposure.

2.2 Experimental Setup and Data Collection

Two different laser systems from IPG Photonics (Oxford, MA) were employed as laser sources for exposure. For the nominal beam diameters of 0.6, 1, and 2 cm, an IPG Photonics YLR-3000 laser with a maximum CW power of 3 kW was used. The experimental configuration for this system has been previously reported.³ Output of this laser from the fiber optic was approximately Gaussian in spatial energy distribution with a $1/e^2$ diameter of ~ 1.3 cm. The size of the beam at target was controlled with the use of a beam expanding/reducing telescope. Power at target was adjusted via electronic control within the laser head via preset PC programming. For each laser exposure, reference energy from a low-power sample of the beam was recorded with a Molectron PM10 power meter (Coherent Inc., Santa Clara, CA). Measurements acquired with the PM10 in the reference beam were compared with measurements obtained with a PM150 placed near the target plane before testing, at the scheduled midway time point during testing and after each sequence of exposures to assure integrity of the high-energy portion of the beam train and to confirm accurate quantification of energy delivered to target. The laser was co-aligned with a helium neon laser (Meredith Instruments, Glendale, AZ) to facilitate beam placement at the target. Beam size at target was measured with a Pyrocam III (Spiricon, Logan, UT) at the time of setup for the 2-cm beam configuration, while burn paper was used to measure the smaller 0.6- and 1-cm-diameter beams. Output from the telescopes was collimated to maintain beam diameter over the expected range of target distances determined from the anatomical confirmation of the animals. Consistency of the beam size was verified during testing with burn paper (ZAP-IT™, Kentek Corporation, Pittsfield, NH). A Sony (San Diego, CA) CCD-Iris color video camera was also utilized in this arrangement for target position verification. This video camera was mounted on a custom translation stage and was co-focused at a common region of interest of the thermal camera.

For the nominal beam diameters of 2.5, 5, and 10 cm, an IPG Photonics YLR-50000 laser was used. This laser system was limited to a maximum CW power of 30 kW for this study. A telescope was used to adjust the beam's diameter at the target located ~ 305 cm from the fiber head. An optical wedge placed ~ 122 cm in front of the fiber head was used to reflect a portion of the beam to a Spectralon screen ~ 183 cm from the wedge. A camera (Alpha Near Infrared InGaS ICI NIR) was aimed and focused at the Spectralon screen to capture the beam's profile using Spiricon software. This allowed for visualization of the beam's profile equidistant to the target without damaging equipment. A Coherent PM150x read by a LabMax power meter was

placed near the Spectralon screen to detect a small portion of the beam to capture the reference arm power with each exposure. To calibrate the energy delivered to the target, a series of energy measurements were taken at the start and end of each day using a Black Ball 3 DELE-S-GP-3 and Coherent PM5K with an EPM2000 power meter. A FLIR SC660 long-wave IR camera was used in this setup to monitor the placement of the subject in addition to providing initial skin surface temperatures.

Pulse widths were verified once at the start of the setup for all of the experiments for both the utilized laser systems. This was done with a silicone photodiode and a TDS3054B or a TDS220 digital oscilloscope (Tektronix Inc., Beaverton, OR). Once it was determined, the laser consistently gave the programmed pulse width; it was not measured again. The oscilloscope showed rise and fall times for the IPG lasers were <100 μ s, providing better than ± 0.5 ms accuracy on the exposure times. Repeated shots were measured with the Coherent PM series thermopile detectors (PM5K, PM10, or PM150 depending on beam size and power configurations) and one of the following Coherent meters operating in energy mode: EPM1000, EPM2000, 3Sigma, or a LabMax.

All energy meters and detectors were verified to have been calibrated by the manufacturer within the year prior to the experiments. Uncertainty on the energy measurements was determined from the specifications from the manufacturer (Coherent) for each of the power meters and power detectors used in the calibration of the beam configuration. This was determined to be $\pm 5.5\%$ for beam diameters <9 cm. Since the largest beam diameter exceeded the detector sizes available, the Black Ball was used to calibrate the energy at the target plane, yielding an uncertainty in delivered energy of $\pm 7.2\%$ for the largest beam diameter condition in the study. The uncertainty associated with the beam diameter was determined by taking the average of the measured standard deviations from multiple beam profiles analyzed from each beam configuration finding a $\pm 2.8\%$ (min and max were 1.1 and 5.2% found for the 9.5 and 0.6 cm beam diameter configurations, respectively).

To capture the temperature rise during and after laser exposure, both laser setups used an SC4000 (IR) high frame rate thermal camera (FLIR Systems, Boston, MA), which is sensitive to radiation in the 3- to 5- μ m thermal emission band. This camera sensitivity was specifically selected to be out-of-band for the 1070-nm wavelength under test so that surface temperature changes during laser exposure could be obtained without backscatter from the target distorting the measurements. The thermal camera was triggered for data collection to begin at least 100 ms prior to laser exposure of the pig skin. IR camera frame rates were 400 fps for experiments where beam diameters were <2 cm and 200 fps for experiments where the beam diameters were >2 cm. The camera collected data for a period of time between 2 and 30 s beyond the completion of each laser exposure to capture the trajectory of thermal decay of the laser-heated tissue. Course focus of the thermal camera was verified with visible feedback from a monitor connected to a video camera.

2.3 Statistical Analysis

The Probit procedure²¹ was used to estimate the ED₅₀ dose (i.e., damage threshold for a lesion in 50% of the observations) for creating an MVL for all laser configurations used in the skin studies at both 1- and 24-h time points. Observers were

instructed that a lesion was constituted as any change in the appearance of the surface of the skin to include any erythema, no matter how slight, blistering, or change in pigmentation as viewed by eye. An exposed area was deemed a lesion if at least two out of three trained observers, blinded from each other, agreed there was a lesion. A minimum of three animals were used for each laser configuration investigated. In addition, 95% confidence intervals for dose response were calculated from the data. An adequate number of data points were collected to ensure that the magnitude of upper and lower fiducial limits at the ED₅₀ level varied no more than 50%. In order to reduce the number of subjects needed, this requirement for the fiducial limits being within 50% of the ED₅₀ was disregarded for the beam diameters >2 cm. Furthermore, a Probit-curve slope greater than two, with aggregated 24-h observation data, was set as a minimal experimental endpoint for the MVL.

3 Results

A total of 1306 skin exposures were completed on both flanks of 22 Yucatan miniature pigs with the 1070-nm laser. Sixteen different configurations of laser parameters were used as listed in Tables 2 and 3 along with correlating ED₅₀'s, Probit slopes, average irradiance, and peak radiant exposure data. It should be noted that the beam diameter is listed as 4σ and not the usual 1/e or 2σ because the 1/e² diameter must be used to evaluate the hazards of laser beams on an average irradiance

basis. The radiant exposure is calculated using peak power, 1/e diameter, not the average which uses 1/e² diameter.

Lesions created from exposure durations <100 ms were typically absent at 1 h and present at 24 h post exposure. Exposure durations ≥100 ms were typically observed at the 1-h read and persisted at 24 h. This general observation is supported by comparing the number of yes/no lesions (column 1 in Tables 2 and 3) at 1 and 24 h post exposure and the ratio of the 1-h ED₅₀ to the 24-h ED₅₀.

To calculate the ratio of ED₅₀:MPE reported in Table 3, the ANSI Z.136.1-2007 standard for the Safe Use of Lasers recommends that for a skin exposure, the limiting aperture should be referenced to a standard 0.35 cm. Thus to compare the experimentally determined ED₅₀'s to the MPE, the irradiance values were scaled to an effective irradiance, E_f , by

$$E_f = \frac{4\Phi_0}{\pi D_L^2} \left[1 - \exp\left(\frac{-D_L^2}{D_f^2}\right) \right], \quad (1)$$

where Φ_0 is the power in Watts, D_L is the 1/e laser beam diameter in centimeter, and D_f is the limiting aperture of 0.35 cm. It is worth noting that for beam diameters > ~1 cm (1/e² diameter), the exponential portion of Eq. (1) begins to approach zero, showing that E_f and the experimentally determined ED₅₀ are nearly the same for these larger beams. Graphical comparison of E_f versus exposure time is contrasted to the MPE in

Table 2 Probit data results from observations for lesions 1 h after exposure from the 1070-nm laser.

1-h Probit						
Number of exposures (Yes, No)	1/e ² diameter (cm)	Time (s)	ED ₅₀ (95% Conf. Inter.) (J)	Probit slope	Irradiance (W/cm ²)	Peak radiant exposure (J/cm ²)
21, 101	0.6	0.01	6.6 (5.7 to 8.3)	5.9	2498	50
27, 27	0.6	0.07	12.7 (11.4 to 14.1)	18.1	687	96
32, 112	0.6	10	58.4 (53.6 to 67.1)	7.6	22	442
45, 146	1.1	0.01	17.3 (15.7 to 19.9)	6.0	1998	40
74, 67	1.1	0.1	22.7 (21.2 to 24.4)	10.7	262	52
73, 71	1.1	10	77.4 (71.9 to 82.7)	10.3	9	179
37, 17	1.9	0.05	58.2 (51.2 to 63.8)	12.1	402	40
47, 83	1.9	0.25	77.9 (74.9 to 81.9)	15.5	108	54
46, 47	1.9	10	162.0 (152.0 to 171.0)	18.0	6	112
19, 22	2.4	0.01	53.6 (29.6 to 92.3)	3.4	1165	23
23, 13	2.4	0.025	40.5 (29.8 to 54.3)	6.5	352	18
27, 12	2.4	0.25	54.8 (40.5 to 68.5)	9.5	48	24
11, 18	4.7	0.025	315.0 (241.0 to 660.0)	8.4	723	36
19, 11	4.7	0.1	283.0 (233.0 to 318.0)	18.0	162	32
33, 7	4.7	0.25	325.0 (229.0 to 372.5)	12.0	75	37
12, 6	9.5	0.25	1142.5 (227.0 to 1367.5)	11.4	65	33

Table 3 Probit data results from observations for lesions 24 h after exposure from the 1070-nm laser. Note the ratio of the ED₅₀ to maximum permissible exposure (MPE) is taken as E_f/MPE , where E_f is the effective irradiance computed from Eq. (1).

24-h Probit							
Number of exposures (Yes, No)	1/e ² diameter (cm)	Time (s)	ED ₅₀ (95% Conf. Inter.) (J)	Probit slope	Irradiance (W/cm ²)	Peak radiant exposure (J/cm ²)	Ratio of ED ₅₀ to MPE
52, 71	0.6	0.01	4.0 (3.8 to 4.3)	13.3	1518	30	13
31, 22	0.6	0.07	11.1 (9.7 to 12.0)	11.7	600	84	22
38, 105	0.6	10	57.1 (52.0 to 65.9)	6.6	22	432	32
46, 143	1.1	0.01	16.1 (15.1 to 17.4)	9.5	1859	37	21
71, 69	1.1	0.1	22.6 (20.5 to 24.6)	6.7	261	52	17
67, 78	1.1	10	82.0 (76.0 to 87.9)	9.3	9	189	19
43, 9	1.9	0.05	48.6 (42.5 to 53.9)	16.3	336	34	13
56, 73	1.9	0.25	74.2 (71.8 to 77.1)	18.9	103	51	13
44, 47	1.9	10	154.0 (142.0 to 166.0)	10.8	5	106	11
24, 17	2.4	0.01	46.6 (38.4 to 53.7)	15.7	1013	20	12
22, 14	2.4	0.025	43.0 (32.3 to 58.0)	7.0	374	19	9
27, 12	2.4	0.25	55.3 (42.3 to 69.3)	11.5	48	24	6
21, 9	4.7	0.025	213.3 (146.3 to 260.0)	7.6	490	24	11
10, 30	4.7	0.1	267.0 (214.0 to 305.0)	13.4	153	31	10
35, 5	4.7	0.25	295.0 (185.0 to 345.0)	11.4	68	34	9
13, 5	9.5	0.25	1125.0 (500.0 to 1310.0)	24.6	64	32	8

Fig. 2. Excel (Microsoft Office 2007) was used to determine the equation to best fit the data for E_f versus t , for each beam diameter and the power fit equation $E_f = at^m$ finding $a = 143.1, 102.7, 65.9, 25.6,$ and 41.8 and $m = -0.63, -0.76, -0.79, -0.94,$ and -0.86 for the 0.6, 1.1, 1.9, 2.4, and 4.7-cm beam diameters, respectively. Note that for this wavelength, the

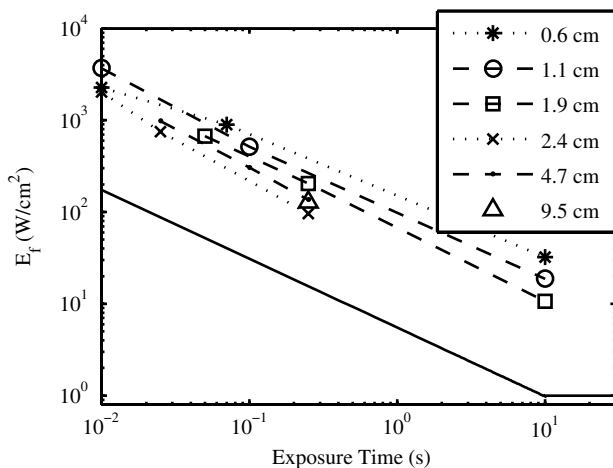


Fig. 2 Damage threshold data converted to the effective irradiance contrasted to the maximum permissible exposure (solid line).

current MPE = $5.5t^{-0.75}$ between 0.01 and 10 s then is a constant 1 W/cm² for exposure durations ≥ 10 s.¹

For exposures very near or above the ED₅₀, a raised appearance known as a wheal (also spelled weal) or flare was commonly observed for lesions at all durations and spot sizes. The raised area on the skin appeared more subtle for exposures near the ED₅₀ and more pronounced for exposures significantly higher than the ED₅₀. The wheal and flare appeared to be proportional to the size of the beam, which was easily visualized by illuminating the lesion at a glancing angle to the skin. The wheal was not always easily visualized when illuminated under general overhead lighting conditions. An example of skin-lesion appearance over observational endpoints is shown in Fig. 3. Black marker grid lines drawn on the skin in Fig. 3 were $\sim 4 \times 4$ cm apart. Though there is no pictorial documentation available, the exposed area appeared red immediately after the laser exposure, but had resolved completely by 1 h. No annotations were made of when the wheal and flare began to appear in any exposures, just that it was observed at 24 h post exposure. Note that the wheal was not used as an indicator for an MVL, but was a general observation reserved for discussion.

IR camera data proved exceptionally difficult to process for this wavelength due to hot spots from the absorption of laser energy in the hair and steam rising from the skin due to phase changes in the water inside the skin. IR camera data for the 0.6- and 1.1-cm beam diameters with exposure durations

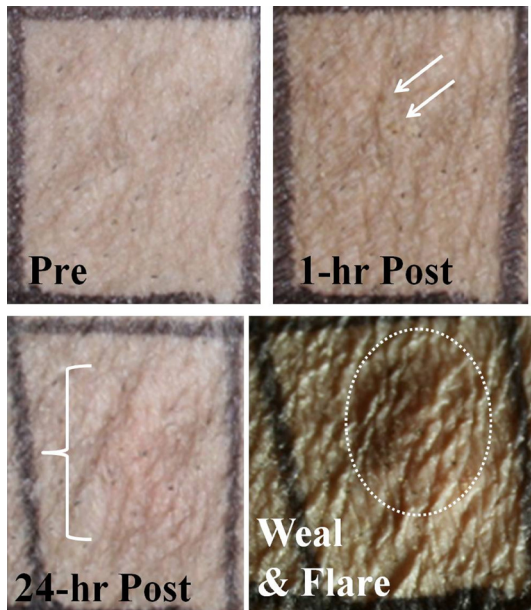


Fig. 3 Example of skin lesions observed in this study before and after laser exposure (10 ms exposure, 2.4 cm beam diameter, $86 \text{ J} \pm 5.5\%$, 1.8 times higher than the 24-h ED_{50}). Both the 1- and 24-h post laser exposure reads were positive for a lesion. The white arrows indicate a very slight brown discoloration on the epidermis; no erythema was observed at 1 h. The white bracket indicates the extent of the observed erythema at 24 h. The dashed, white circle approximates the footprint of the observed raised area on the skin 24 h post exposure.

<10 s were processed, but had enormous variability during laser heating due to these superficial hot spots and were not suitable for rate-of-heating analysis.

IR camera data were processed by selecting a region of interest (ROI) (typically 9 to 20 pixel diameters) placed in the central area of exposure to examine the averaged temperature in the ROI at each time t during the laser exposure ($0 < t \leq$ exposure duration) and after the laser was turned off ($t >$ exposure duration). Since hair burns very quickly at this wavelength, care was taken to avoid hot spots believed to be follicles, or in some cases, steam, sometimes requiring the ROI to be parsed into two smaller 3 by 3 pixel ROIs. The initial temperature, T_0 , of the exposed skin surface was determined from IR camera data acquired before the laser turned on ($t \leq 0$). The change in temperature, ΔT , was then determined by the difference between T_0 and the peak temperature, T_{peak} , at the end of the exposure. IR camera data were processed to give the linear relationships, with a forced zero intercept, for the peak temperature rise, ΔT , as a function of power P . The ΔT versus P data for the 1.9-cm beam diameter are shown in Fig. 4. The slopes, m_T , were recorded from each fit to processed thermographic data for $\Delta T = m_T P$ and are reported in Table 4.

The average and standard deviation for T_0 at each exposure condition shown in Fig. 4 are also reported in Table 4. The slopes in Table 4 are also corrected for radiant exposure by $m_T \times (\pi d^2/4t)$ [$^{\circ}\text{C}/(\text{J}/\text{cm}^2)$] for later discussion.

Time-temperature history for each of the three beam diameters in the 10-s exposures near ED_{50} are shown in Fig. 5(a). The periodic ripples in the 10-s exposures stem from the subject's breathing; care was taken to keep the ROI in the central area of the beam to minimize the variations induced by the

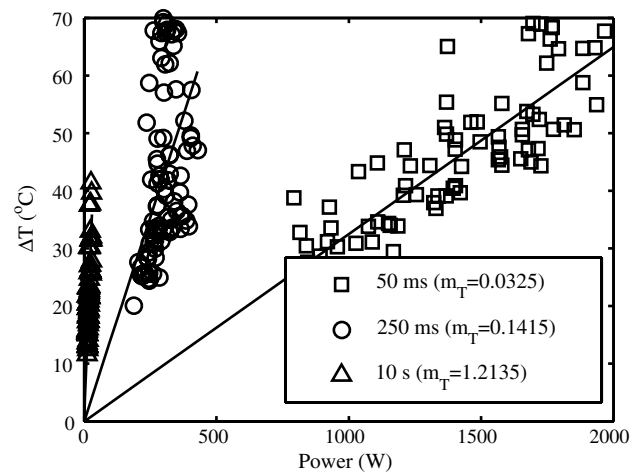


Fig. 4 The peak temperature rise from numerous exposure powers for the 1.9 cm beam diameter as tested at 0.05, 0.25, and 10 s exposure durations. Units on the slope fit parameter, m_T , are $^{\circ}\text{C}/\text{W}$.

breath (i.e., hair follicles/hot spots moving periodically through the ROI).

Time-temperature history for tested cases nearest ED_{50} for the largest beam diameter (250 ms, 9.5 cm) and shortest exposure (10 ms, 2.4 cm) are shown in Fig. 5(b). Notice that the experimentally determined m_T ($^{\circ}\text{C}/\text{W}$) in Table 4 for these two exposure duration-diameter pairs [depicted in Fig. 5(b)] are the same in $^{\circ}\text{C}/\text{W}$, but very different in $^{\circ}\text{C}/(\text{J}/\text{cm}^2)$. All time-temperature curves presented in Fig. 5 were positive for a lesion at 24 h. It should be noted that the uncertainty of the energy measurements was $\pm 5.5\%$ for all beam diameters <9 cm and $\pm 7.2\%$ for the 9.5-cm beam reported in Figs. 5 and 6.

The thermal video files corresponding to the time-temperature histories depicted in Fig. 5(b) for the 2.4- and 9.5-cm cases are shown in Video 1 and Video 2. Figure 6 shows still frames of the supplemental video files for the thermal images captured nearest to the laser's cutoff time.

Analyzed thermal data for the 2.4-cm beam at the 10-ms pulse did not necessarily capture the peak temperature (200 fps, 1.5 ms integration time); thus these data were analyzed differently than all other thermal data by using the two frames where the laser was on, selecting an ROI in frame 1 to find the temperature rise ΔT_1 at t_1 and then the same ROI in frame 2 to find ΔT_2 at t_2 . A linear fit was then applied to the thermal data to identify ΔT as function of time and solving the linear fit for an assumed ΔT_{max} at $t = 10$ ms (having assumed $\Delta T = 0$ at $t = 0$). Most of these 10-ms data only had two frames showing increasing temperature, but one 2.4-cm, 10-ms thermal video captured three frames showing increasing temperature, giving some experimental evidence of the peak temperatures achieved nearest the end of this laser pulse. This uniquely captured event is presented as supplemental data Video 1.mp4 (43 kB); the time stamp in the video was created with the assumption the peak temperature profile occurred at $t = 10$ ms. Discussion about when the peak temperature may occur from a 10-ms pulse is reserved for later.

Histology sections of Yucatan miniature pig skin punch biopsy samples were prepared with haematoxylin and eosin staining. Punch biopsies were collected from the central grid area to coincide with the center of the laser exposure site.

Table 4 The linear slopes, m_T , ($^{\circ}\text{C}/\text{W}$) from the fitted thermal camera data $P(\Delta T)$ and calculated ΔT_{MVL} to achieve the minimum visible lesion at 24-h ED_{50} 's.

Exposure duration, t (s)	$1/e^2$ diameter, d (cm)	m_T ($^{\circ}\text{C}/\text{W}$)	Goodness of linear fit to data, R^2	$[(m_T \pi d^2)/4t]$ ($^{\circ}\text{C}/(\text{J}/\text{cm}^2)$)	T_0 ($^{\circ}\text{C}$)	$\Delta T_{\text{MVL}} = m_T (^{\circ}\text{C}/\text{W}) \times \text{ED}_{50,24\text{-h}}$ (W)
0.01	2.4	0.0065	0.778	2.99	33.5 ± 0.5	30.3
0.025	2.4	0.0174	0.858	3.20	33.8 ± 0.6	29.9
0.05	4.7	0.0040	0.800	2.79	34.3 ± 0.7	34.1
0.05	1.9	0.0310	0.561	1.80	31.7 ± 2.1	30.1
0.1	4.7	0.0119	0.691	2.07	33.4 ± 0.7	31.8
0.25	1.9	0.1162	0.324	1.35	31.9 ± 1.0	34.5
0.25	2.4	0.0996	0.983	1.83	33.7 ± 0.4	22.0
0.25	4.7	0.0221	0.943	1.54	31.6 ± 2.0	26.1
0.25	9.5	0.0065	0.638	1.82	32.9 ± 1.2	29.3
10	0.6	3.1175	0.545	0.08	32.2 ± 0.7	17.8
10	1.1	2.4735	0.683	0.21	27.0 ± 2.6	20.3
10	1.9	1.3144	0.841	0.38	35.2 ± 1.9	20.2

Biopsies taken from unexposed areas of skin on the flank were used to measure skin thicknesses. Thicknesses of the stratum corneum (SC), epidermis (not including SC), and dermis ranged from 14 to 47, 52 to 82, and 2350 to 3860 μm with averages and standard deviations of 29 ± 10 , 59 ± 17 , and 2953 ± 153 μm , respectively. Histological evaluations of the damage lesions are reserved for a future paper.

4 Discussion

MVLs are considered to be any subtle, slight, morphological or coloration change observed at the exposure site post laser radiation at 1- and 24-h time points. These changes include the faint brown discoloration or reddening (depicted in Fig. 3), or more obvious changes such as blistering or charring. Blistering and/or

charring of the skin were not observed at the ED_{50} level for any exposure condition in this study. The MVL does not necessarily describe persistent, irreparable damage to the tissue, but rather provides evidence for radiant energy levels that will begin to cause noticeable changes to the tissue, with some changes being transient in nature.

Laser-induced erythema and wheal and flare appear to have a transient, and perhaps related, nature that is not well understood. It was common to observe immediate erythema, which disappeared at 1 h, but reappeared at 24 h post exposure for the 10-ms cases (Fig. 3). This is in contrast to 250-ms cases of the same beam diameter where disappearing erythema at 1 h usually remained resolved at 24 h. Foster et al.²² reported the curious ability of erythema caused by 1320/1440-nm laser

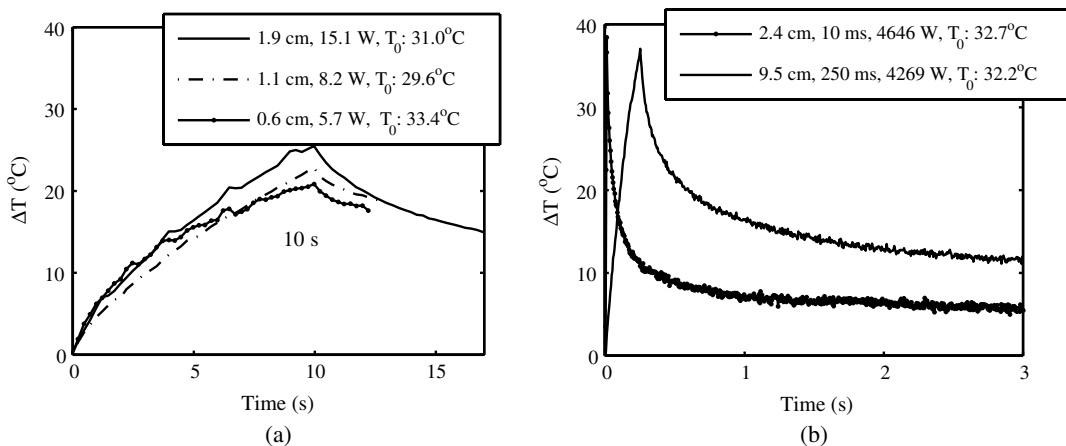


Fig. 5 Time-temperature history for cases nearest ED_{50} resulting in a lesion at 24 h for (a) 10-s exposures, various beam diameters, and (b) largest beam diameter (9.5 cm) contrasted to the shortest exposure (10 ms) condition tested.

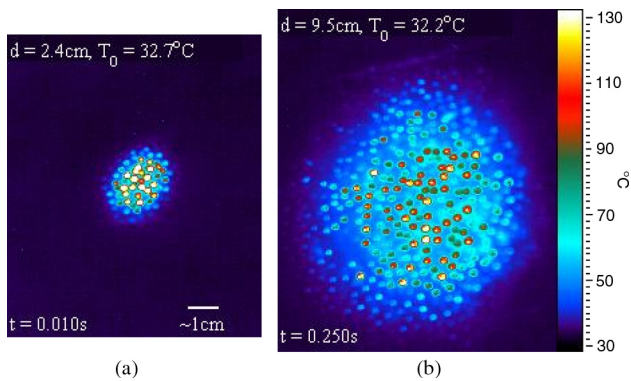


Fig. 6 The thermal image captured at the end of laser exposure of cases nearest 24-h ED_{50} for (a) 2.4 cm diameter, 10 ms, 46.5 ± 2.6 J (Video 1, MP4, 43 kB) [URL: <http://dx.doi.org/10.1117/1.JBO.19.3.035007.1>] and (b) 9.5 cm diameter, 250 ms, 1067 ± 77 J (Video 2, MP4, 137 kB) [URL: <http://dx.doi.org/10.1117/1.JBO.19.3.035007.2>]. The laser comes on at $t = 0$. Temperatures are absolute T ($^{\circ}\text{C}$). The 1-cm scale bar applies to both (a) and (b).

radiation to resolve after 24 h, then reappear upon subtle thermal stimulation (i.e., hot shower) 48 h after exposure, and suggested this recall ability may be related to the wheal and flare response. Wheal and flare was observed at exposure levels at or above damage threshold for all laser beam diameters and exposure times in this study. The observation of the wheal and flare from exposed areas at or above damage threshold is not uncommon for laser exposures to skin in the visible or IR.^{23–26} The wheal and flare is believed to be a neurogenic response caused by the stimulation of a neuropeptide protein called Substance P (SP).^{23,24} The exact mechanism of how and why the laser stimulates SP is not known, though one hypothesis proposed by Algermissen et al.²⁶ suggests this involves the thermal destruction of the nerve endings in the dermis and/or epidermis from the laser exposure. The wheal and flare has not been used as an indicator of the MVL, though it should be included in future studies as part of the observational evidence lending insight into the tissue response at damage threshold exposure levels.

Comparing the MPE to the effective irradiances, E_f , used in this study found that the margin for safety between the E_f and MPE ranges from a ratio of 6.2 to >32.3 (last column in Table 3). The data trends in Fig. 2 indicate that the damage threshold may have a weak dependence on beam diameter much larger than the 0.35-cm limiting aperture used in the ANSI.¹ For the 0.25-s exposures, the 1.9-cm beam had a statistically significant higher threshold (51.26 J/cm²) than the larger beam diameters, indicating that the threshold is dependent on beam diameter, at least for $d < 2$ cm (Fig. 2). The 2.4-, 4.7-, and 9.5-cm beam diameters converged toward a peak radiant exposure threshold level of ~ 30 J/cm² as indicated by their significantly overlapping 95% confidence intervals. This suggests that for 0.25-s exposures at 1070 nm, the peak radiant exposure threshold converges to ~ 30 J/cm², settling to a safety margin (ratio of E_f :MPE) of ~ 8 , for $d > 2$ cm. The 0.1-s did not have overlapping 95% confidence intervals for peak radiant exposure thresholds of 52.2 and 30.65 J/cm² for the 1.1- and 4.7-cm beam diameters, respectively. If the evidence for convergence to ~ 30 J/cm² in the 0.25-s data is considered, it is likely that the threshold for the 4.7-cm case represents a value for convergence between threshold and increasing beam diameters for 0.1-s exposures, giving a safety margin of ~ 10 between

threshold E_f and MPE for very large beam diameters. The 10-s exposure data, however, were 432.24 , 189.4 , and 106.38 J/cm² for the 0.6-, 1.1-, and 1.9-cm beam diameters, respectively, and exhibit no overlap in 95% confidence intervals, suggesting that convergence of the threshold with respect to beam diameter was not achieved. The larger spread in damage thresholds for the 10-s data also suggest that damage threshold is more dependent on beam diameter for very long exposures compared to exposures < 10 s. The 0.01-s exposure thresholds for the 0.6- and 1.1-cm diameters have overlapping confidence intervals, but the larger 2.4-cm beam diameter had a peak-radiant exposure damage threshold 33% less than the smaller beams, suggesting some dependency on beam diameter even for this very short exposure. These trends in beam diameter dependency for MVL threshold data are suspected to be caused by different damage mechanisms for very short exposures (< 0.05 s) compared to the longer exposure durations.

The nature of skin lesions generated with 1070-nm laser radiation is, in general, markedly different from those generated with longer IR wavelengths, such as 1940 nm. This difference is readily observed at shorter-duration exposures. Lesions generated from the 1070-nm wavelength for short (10-ms) exposure durations and smaller diameters (0.6 and 1.1 cm) seemed to be multifocal in nature and involved a desiccation process as evidenced by a white, flaky appearance to the lesion, whereas MVL studies of lesions from the 1940-nm wavelength do not report this characteristic.^{3,27} The 1070- and 1940-nm laser radiation wavelengths have significantly different damage thresholds in skin at comparable conditions. For example, Oliver et al.³ reported a 1940-nm wavelength with a 1.8-cm, 10-s exposure had a 24-h ED_{50} of ~ 13.3 J/cm² on Yucatan mini-pig skin, as compared to the 1070-nm wavelength using a 1.9-cm, 10-s exposure, which had an ED_{50} of 106.3 J/cm², eight times that of a comparable setting at the longer 1940-nm wavelength. These differences in lesion appearance and damage thresholds at comparable conditions between the 1940- and 1070-nm laser radiations can be explained by differences in optical absorption and scattering of melanin and water in the skin.

Based upon the literature cited in Table 1, damage thresholds at 1070 nm should be highly dependent upon pigmentation. The absorption of pigment should be considered up to wavelengths of ~ 1400 nm, where absorption in bulk tissue should become substantially less significant than water absorption due to the low fractional content of pigment as compared to the surrounding water content. The consistency of pigmentation between Yucatan miniature pigs used in this aspect of the study likely helped minimize variance of data. Rockwell and Goldman¹⁵ and Baozhang et al.¹⁰ have reported thresholds for darker skin to be as much as 20 to 25% lower than lighter-skin subjects when using a 1064-nm wavelength. This is in stark contrast to studies at the 1940-nm wavelength by Chen et al.,²⁸ which do not report significant differences in thresholds between light- and dark-pigmented skin. If the 24-h ED_{50} MVL is $\sim 25\%$ lower for darker skin exposed to 1070-nm laser radiation, then the safety margin between E_f and MPE would reduce significantly to a range of 1.5 up to 8.1. Adequacy of the animal model should be considered when applying these findings to all pigmentation levels expected across the human race and sufficient safety margins should take this variation into account.

The 1070-nm laser radiation wavelength also penetrates deeper into tissue, heating a larger volume, as compared to the 1940-nm wavelength. When comparing the thermal burn

created by a 1064-nm laser radiation wavelength (1 cm beam diameter, 40 W delivered for 8 s) to a copper-brass iron, Zhang et al.²⁹ reported tissue damage through the skin into internal organs of a Wistar rat model where lesions had a coagulative burn appearance on the skin surface. Though the dorsal skin of the Wistar rat was significantly thinner and had far less subcutaneous tissue than the Yucatan mini-pig model, the observations reported in Zhang et al.²⁹ demonstrated the deeply penetrating nature of this laser radiation wavelength region. It is this very nature of these deeply penetrating wavelengths that is believed to give rise to the MVL threshold dependency on beam diameter. This wavelength heats a larger volume of tissue, compared to less penetrating wavelengths, enabling radial conduction to dominate over axial thermal diffusion.

Vapor or smoke was observed for some of the higher-energy exposures near or above threshold, particularly for the 10-ms exposures, providing evidence for water phase transitions occurring in deeper layers of the skin. On occasion, dry skin debris would explode off the surface (popcorn effect) when exposed to short exposures (<100 ms). However, these seemingly violent interactions did not always result in grossly observable damage to the skin surface. Due to better penetration at 1070 nm, the heat source generated by this laser within the tissue has a significantly larger volume than that generated at longer wavelengths where water absorption dominates. It is possible that the peak temperature of the skin surface occurs a few milliseconds after a 10-ms, 1070-nm laser exposure has concluded. This is feasible because the tissue beneath the surface heats rapidly, and potentially, to a higher temperature than the surface due to multiple scattering events and elevated subsurface fluence levels. Under such conditions, the thermal diffusion time required for heat to propagate to the surface would cause the peak temperature observed at the surface of the skin to occur after a sufficiently short exposure has ceased. The thermal confinement time at this wavelength can be quite long, especially for large-diameter beams. As a result, the build-up of pressure from steam generated in the volume of tissue can cause superficial dry skin to explode off the surface. This observation may reveal that there is a transition in surface damage processes with lasers operating near 1070 nm for exposure durations much longer (milliseconds versus microseconds) than typically associated with photomechanical damage.

Analysis of thermal video data revealed the thermal slopes, m_T (Table 4), which described the linear relationship between the temperature rise, ΔT , per Watt delivered to the exposure cite (Fig. 4) for a given exposure duration and beam diameter. Variance in the thermal data can be attributed to the angle of incidence from laser exposure (i.e., curved surface of flank), and water and melanin content in the skin. This linear relationship assists in understanding the tissue response. For instance, the m_T for the 10-ms, 2.4-cm group and 250-ms, 9.5-cm group were both 0.0065°C/W (Table 4) and had similar peak temperatures at damage threshold ($\Delta T_{MVL} \sim 30^\circ\text{C}$), but when the thermal slope was corrected for radiant exposure, the two exposure conditions were 2.99 and 1.82°C/(J/cm²), respectively. Furthermore, the thermal slopes for the 10-s exposures revealed that the ΔT_{MVL} was $\sim 20^\circ\text{C}$, significantly lower than the $\sim 30^\circ\text{C}$ temperatures found for most other exposures <10 s. This is consistent with thermal data analysis from a 1319-nm laser radiation skin damage study, which also found ΔT_{MVL} for 10-s exposures to be $\sim 20^\circ\text{C}$.⁷ These thermography data may provide evidence for the rate of reaction as a function of peak temperature when combined with mathematical modeling.

Computational models of laser-tissue interaction traditionally use the Arrhenius equation to simulate the reaction rate of the processes with the model forced to estimate damage at time points at or very near the end of the laser exposure.³⁰ However, the experimental damage threshold is assessed at 1 and 24 h, much beyond the exposure duration of the laser. The appearance of lesions at the 24-h end point is complicated by numerous poorly understood pathways resulting in such sequelae as neurogenic inflammation and disappearing/reappearing erythema. When combined with computational models of laser-tissue interaction, these thermographic data (Table 4) will help to better understand the processes involved in lesion formation. Computational models of the data presented here are in progress.

Thermography data showed that regardless of exposure duration and beam diameter, hair follicles always reached higher temperatures than surrounding skin, but observation of lesions did not center around, nor seem directly related to, the follicle cites or the observation of vapor or smoke. The Yucatan minipigs used in this study had black colored hair, which always appeared darker in contrast to subjects' skin. Hair that had not been effectively removed by clipping appeared to burn upon exposure with high irradiance levels. For example, consider the time-temperature histories presented in Fig. 5(b) where thermal camera images (Video 1 and Video 2) showed follicular cites reaching absolute temperatures in excess of 130 + °C (camera saturation) while the skin in between these hot follicles peaked near 70°C. For the 9.5-cm, 250-ms case, the lowest energy tested was about half the ED₅₀ (thermal data not shown) and still caused the hair follicles to reach 120 + °C, but no lesion was observed. For a 2.4-cm, 10-ms case using a power at 980 W (a factor of 4.7 times less than the ED₅₀ of 4660 W), slight follicular hot spots were observed to reach $\sim 41^\circ\text{C}$, only $\sim 4^\circ\text{C}$ higher than the skin peak temperature. However, a 2.4-cm, 10-ms case at 1236 W (a factor of 3.7 times less than the ED₅₀) showed follicular hot spots beginning to appear with a follicle peaking at $\sim 54^\circ\text{C}$ while the skin peaked at $\sim 40.0^\circ\text{C}$. When the 10-ms, 2.4-cm exposure was about half of the ED₅₀, some follicles peaked above 90°C while the skin peaked at $\sim 49^\circ\text{C}$. Thermal data from these lower-power 10-ms, 2.4-cm cases indicate the hair residing in the follicle had a thermal slope, m_T , between three and five times greater than the m_T for skin in this study.

5 Conclusion

For 1070-nm skin exposures, beam diameters >2.5 cm seem to have a weak to no effect on threshold radiant exposure levels for exposure times between 0.01 and 0.25 s, but may have a larger effect on thresholds for exposures ≥ 10 s. The MVL thresholds beam diameter dependency for 0.01 s is not well understood, but is suspected to involve photomechanical damage mechanisms confounded by the large volume, especially for larger beam diameters, of tissue heated very quickly by this wavelength. At 1070 nm, damage threshold values determined in this study indicate that a buffer of at least a factor of six in the MPE as defined by the ANSI Standard 2007 (Ref. 1) exists, with higher levels of protection afforded by the standard at smaller beam diameters. These margins of safety are consistent with those reported in the literature for the pigmented pig skin at other near-IR wavelength bands between 1000 and 2000 nm.

Acknowledgments

The authors would like to thank the staff of the Air Force Research Laboratory Veterinary Sciences Branch (711 HPW/RHDV) for their expert animal care and handling service and Robert Ulibarri and Shane Johnson from the Directed Energy Effects Branch (AFRL/RDLE) for training support and the use of their laser and diagnostics assets. The authors would also like to thank J. Michael Rickman for his help in making video files, Justin Zhoner, Doug Goddard, Michael Foltz, and Victor Villavicencio for helping with logistics for the experimental setup and data collection, and Michael Wyche, Isaac Noojin, and Andrew Wharmby for thermal video processing. Research performed by TASC Inc. was conducted under USAF Contract Numbers F41624-02-D-7003 and FA8650-08-D-6930.

References

- American National Standards Institute "American National Standard for safe use of lasers," in *ANSI Z136.1*, pp. 62–66, 76–78, Laser Institute of America, Orlando, FL (2007).
- T. A. Eggleston et al., "Comparison of two porcine (*Sus scrofa domestica*) skin models for in vivo near-infrared laser exposure," *Comp. Med.* **50**(4), 391–397 (2000).
- J. W. Oliver et al., "Infrared skin damage thresholds from 1940-nm continuous-wave laser exposures," *J. Biomed. Opt.* **15**(6), 065008 (2010).
- J. W. Oliver et al., "Skin damage thresholds with continuous-wave laser exposures at near infrared wavelengths," in *Int. Laser Safety Conf.*, Laser Institute of America, Orlando, FL (2011).
- C. P. Cain et al., "Porcine skin visible lesion thresholds for near-infrared lasers including modeling at two pulse durations and spot sizes," *J. Biomed. Opt.* **11**(4), 041109 (2006).
- C. P. Cain et al., "Visible lesion thresholds with pulse duration, spot size dependency, and model predictions for 1.54-microm, near-infrared laser pulses penetrating porcine skin," *J. Biomed. Opt.* **11**(2), 024001 (2006).
- J. W. Oliver et al., "Infrared skin damage thresholds from 1319-nm continuous wave laser exposures," *J. Biomed. Opt.* **18**(12), 125002 (2013).
- T. L. Troy and S. N. Thennadil, "Optical properties of human skin in the near infrared wavelength range of 1000 to 2200 nm," *J. Biomed. Opt.* **6**(2), 167–176 (2001).
- E. Salomatina et al., "Optical properties of normal and cancerous human skin in the visible and near-infrared spectral range," *J. Biomed. Opt.* **11**(6), 064026 (2006).
- M. W. Baozhang et al., "Study of injury thresholds of CW Nd:YAG laser light for human skin," *Chin. J. Lasers* **12**(10), 582–585 (1985).
- W. Y. Tingbi et al., "Research on injury threshold of Chinese yellow skin by CW Nd:YAG laser beam irradiation," *Chin. J. Lasers* **12**(10), 626–628 (1985).
- W. Y. Tingbi et al., "Research on injury threshold of Chinese yellow skin irradiated with 300 us pulsed neodymium glass laser light," *Chin. J. Lasers* **12**(10), 628–630 (1985).
- L. Zhaozhang, "Laser safety, protection standards reviewed," *Chin. J. Lasers* **6**(3), 141–144 (1986).
- R. R. Anderson et al., "Selective photothermolysis of cutaneous pigmentation by Q-switched Nd: YAG laser pulses at 1064, 532, and 355 nm," *J. Invest. Dermatol.* **93**(1), 28–32 (1989).
- R. J. Rockwell, Jr. and L. Goldman, *Research on Human Skin Laser Damage Thresholds*, pp. 1–148, USAF School of Aerospace Medicine, Cincinnati, OH (1974).
- R. L. P. van Veen et al., "Determination of VIS- NIR absorption coefficients of mammalian fat, with time- and spatially resolved diffuse reflectance and transmission spectroscopy," in *Biomedical Topical Meeting*, 14 April 2004, Miami Beach, Florida, Paper SF4, Optical Society of America, Washington, DC (2004).
- D. J. Segelstein, "The complex refractive index of water," MS Thesis, University of Missouri, Kansas City, Missouri (1981).
- H. E. Arimoto, M. Egawa, and Y. Yamada, "Depth profile of diffuse reflectance near-infrared spectroscopy for measurement of water content in skin," *Skin Res. Technol.* **11**(1), 27–35 (2005).
- A. Roggan et al., "Optical properties of circulating human blood in the wavelength range 400–2500 nm," *J. Biomed. Opt.* **4**(1), 36–46 (1999).
- S. L. Jacques, R. D. Glickman, and J. A. Schwartz, "Internal absorption coefficient and threshold for pulsed laser disruption of melanosomes isolated from retinal pigment epithelium," *Proc. SPIE* **2681**, 468–477 (1996).
- D. J. Finney, *Probit Analysis*, Cambridge University Press, Cambridge, UK (1971).
- K. W. Foster, E. F. Fincher, and R. L. Moy, "Heat-induced 'recall' of treatment zone erythema following fractional resurfacing with a combination laser (1320 nm/1440 nm)," *Arch. Dermatol.* **144**(10), 1398–1399 (2008).
- D. Roosterman et al., "Neuronal control of skin function: the skin as a neuroimmunoendocrine organ," *Physiol. Rev.* **86**(4), 1309–1379 (2006).
- M. Steinhoff et al., "Modern aspects of cutaneous neurogenic inflammation," *Arch. Dermatol.* **139**(11), 1479–1488 (2003).
- J. M. Handley, "Adverse events associated with nonablative cutaneous visible and infrared laser treatment," *J. Am. Acad. Dermatol.* **55**(3), 482–489 (2006).
- B. Algermissen et al., "Laser-induced weal and flare reactions: clinical aspects and pharmacological modulation," *Br. J. Dermatol.* **146**(5), 863–868 (2002).
- B. Chen et al., "Histological and modeling study of skin thermal injury to 2.0 micron laser irradiation," *Lasers Surg. Med.* **40**(5), 358–370 (2008).
- B. Chen et al., "Effect of pigmentation density upon 2.0 micron laser irradiation thermal response," *Health Phys.* **93**(4), 273–278 (2007).
- Y. Zhang et al., "Comparative study of 1,064-nm laser-induced skin burn and thermal skin burn," *Cell Biochem. Biophys.* **67**(3), 1005–1014 (2013).
- S. L. Jacques, "Ratio of entropy to enthalpy in thermal transitions in biological tissues," *J. Biomed. Opt.* **11**(4), 041108 (2006).

Biographies of the authors are not available.